# A Practical and Reliable Solution for the Damage Analysis of Composite Structures, with Applications to Automotive

Michaël Bruyneel, Cédric Lequesne, Benoit Magneville & Michael Hack
Siemens PLM Software

Yuta Urushiyama & Tadashi Naito
Honda R&D

Laminated composite materials have been successfully used in the aerospace industry for years. Today, the automotive sector must produce vehicles that satisfy strong regulations on gas emission. Carbon fiber-reinforced plastics, because of their high stiffness and strength to density ratio, represent a serious alternative to classical metallic approaches but generate the need to revisit the design, structural sizing and manufacturing methodologies of the parts. Concerning structural sizing, composites exhibit complex material behaviours, especially for heavily loaded structures when the assumption of linearity cannot be done anymore. Moreover, composite materials and structures show specific failure modes, which must be well controlled in the structural sizing process to exploit the full capacity of the material. In this context, and in order to reduce the development time and cost, simulation can become an interesting companion to the physical tests in the building block approach (pyramid of tests, Figure 1). There is a need to develop predictive material models able to represent the different modes of degradation of the plies forming the laminate. Delamination, that is the ply separation, must also be taken into account in the problem. The solution available in LMS Samtech Samcef is described in this paper, and demonstrated in the automotive context. Only static computations are carried out in this paper. Fatigue is also briefly discussed.

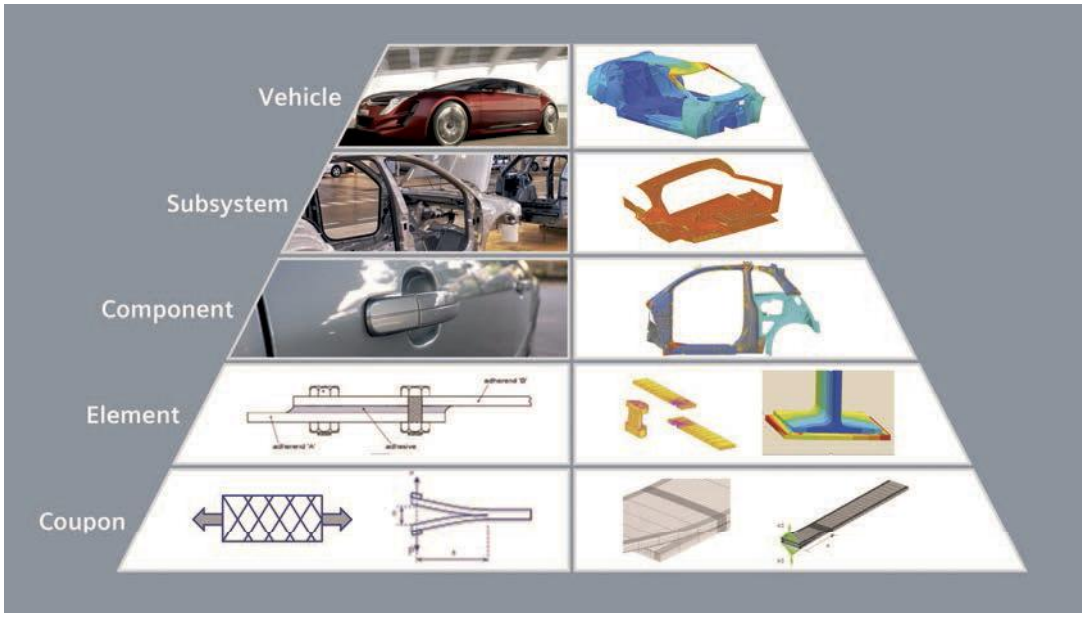


Figure 1. The pyramid of tests: physical and predictive virtual prototypes

## Material Models for Inter and Intra-Laminar Damage

The intra-laminar damage model for the unidirectional ply is described in detail in references [1,2]. It is based on the continuum damage mechanics. In this approach, damage variables taking their values between 0 and 1 are introduced in the formulation to penalize the material stiffness.

The model includes 23 parameters (to be identified): the 9 elastic orthotropic properties in 3D ($E^0_1$, $E^0_2$, $E^0_3$, $\nu_{12}$, $\nu_{23}$, $\nu_{13}$, $G^0_{12}$, $G^0_{13}$, $G^0_{23}$) and specific parameters associated to damage and plasticity (like $Y_{11s}$, $Y_{012}$, $Y_{s12}$, $R_0$, $\beta$ and $n$ in Figures 2 and 3).

The potential $e_d$ in (1), written here in plane stress for the homogeneous ply, includes the damage variables $d_{11}$, $d_{22}$ and $d_{12}$ related to the fibres, the transverse and the shear directions, respectively. The damage in the transverse direction only appears in tension, not in compression, as cracks get closed in the matrix under a compressive loading.

$$e_d = \frac{\sigma_{11}^2}{2(1-d_{11})E_1^0} - \frac{\nu_{12}^0}{E_1^0}\sigma_{11}\sigma_{22} - \frac{\langle\sigma_{22}\rangle_+^2}{2(1-d_{22})E_2^0} + \frac{\langle\sigma_{22}\rangle_-^2}{2E_2^0} + \frac{\sigma_{12}^2}{2(1-d_{12})G_{12}^0} \quad (1)$$

The so-called thermodynamic forces $Y_I$ (see reference [1]) are the derivatives of the potential $e_d$ with respect to the damage variables $d_i$. They can be seen as the loading in the different directions. They manage the evolution of the damages via relations $d_{11}(Y_{11})$, $d_{22}(Y_{12},Y_{22})$ and $d_{12}(Y_{12},Y_{22})$, see Figure 2a and 2c. In the fibre direction (Figure 2a), the behaviour is brittle, and the damage increases suddenly from 0 to 1 when the material strength (expressed in terms of $Y_{11}$) is reached. In the matrix, the damage produces a decrease of the material stiffness (Figure 2b), and its evolution with respect to the loading (here $\sqrt{Y_{12}}$) is more complex (Figure 2c). The two damages in the matrix, $d_{12}$ and $d_{22}$, are coupled.

Besides damage, non-linearity is also taken into account in the fibre direction (Figure 3a). For the matrix, inelastic effects are considered in the form of a plastic law, which captures the permanent deformations (Figures 2 and 3). These material behaviours come from the tests interpretation.

The inter-laminar damage model for delamination is based on cohesive elements [3,4]. A potential is assigned to the interface elements, and three damage variables $d_i$ are related to modes *I*, *II* and *III* (opening, sliding and tearing modes, respectively).

$$e_d = \frac{1}{2}\begin{bmatrix} k_I^0\langle\varepsilon_{33}\rangle_-^2 + k_I^0(1-d_I)\langle\varepsilon_{33}\rangle_+^2 \\ + k_{II}^0(1-d_{II})\gamma_{31}^2 + k_{III}^0(1-d_{III})\gamma_{32}^2 \end{bmatrix} \quad (2)$$

$k_i^0$ in (2) is the undamaged stiffness. Thermodynamic forces $Y_i$ are obtained by deriving (2) with respect to $d_i$. For mixed mode loading, the damage evolution is related to the inter-laminar fracture toughness ($G_{IC}$, $G_{IIC}$ and $G_{IIIC}$) in an equivalent thermodynamic force $Y$ taking the following form:

$$Y = \sup_{\tau\le t} G_{IC}\left\{\left(\frac{Y_I}{G_{IC}}\right)^\alpha + \left(\frac{Y_{II}}{G_{IIC}}\right)^\alpha + \left(\frac{Y_{III}}{G_{IIIC}}\right)^\alpha\right\}^{1/\alpha} \quad (3)$$

In (3), $\alpha$ is a coupling coefficient, and $t$ represents the time (pseudo-time when static analysis is addressed). The *sup* symbol in (3) means that the thermodynamic force can't decrease over time, so reflecting that damage is irreversible. In the model, the three damage variables have the same evolution over the loading and a unique damage $d$ is therefore defined. The damage is related to $Y$ via a function $g(Y)$. Three different functions $g(Y)$ are available leading to exponential, bi-triangular and polynomial cohesive laws.

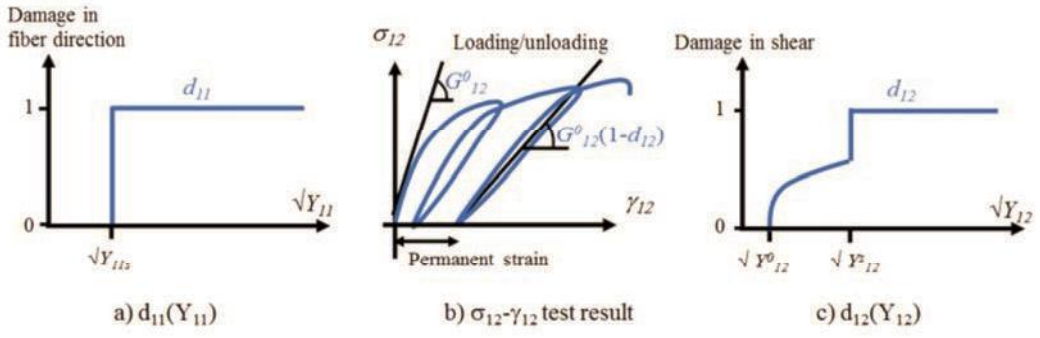


Figure 2. Damages in the fiber direction (left) and in the matrix

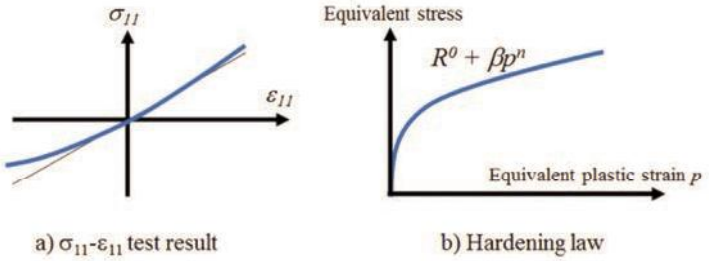


Figure 3. Non linearities in the model

## Parameter Identification Procedure

From the coupon testing performed on classical machines according to some standards (e.g. ASTM D3039, www.astm.org), the longitudinal stress $\sigma_L$ and the axial and transversal strains $\varepsilon_L$ and $\varepsilon_T$ are obtained. Based on this information at the coupon level, the 23 parameters of the ply model are determined. In practice, four series of tests are conducted, each series on a specific (well-defined) stacking sequence and/or loading scenario. As 5 successful tests are usually required, it results that 20 (= 4 x 5) successful tests must be conducted to cover the 4 series, that is a total of 20 tested coupons only. This is enough to identify the 23 parameters of the progressive damage ply model, i.e. the damage, plastic and initial elastic properties. The identification procedure is done without extensive use of simulation. It is a simple procedure based on EXCEL sheets, which can be sped up by some very simple programming. A comparison between an ASTM D3039 test and simulation is used to validate the identified values on a stacking sequence not used for the identification (Figure 4).

For the cohesive laws, specific DCB, ENF and MMB tests (www.astm.org) are performed. Finite element models are developed and a fitting between experiments and numerical results is conducted (Figure 5) to get the value of the parameters. Analytical solutions based on the beam theory are also used to fine tune these values.

## Validation at the Upper Stage of the Pyramid

The previously identified parameters of the inter- and intra-laminar damage models are now used in simulations at the upper stage of the pyramid of Figure 1. Solid shell finite elements with EAS and ANS formulations are used. The element height is equal to the ply thickness. Interface elements are defined between each ply.

In a first application, a [45/0/-45/90]s plate is submitted to an impact. Test results are obtained with a C-scan. The simulation determines the amount of damage in each interface; red meaning completely broken while blue corresponds to no local damage. The damaged interfaces

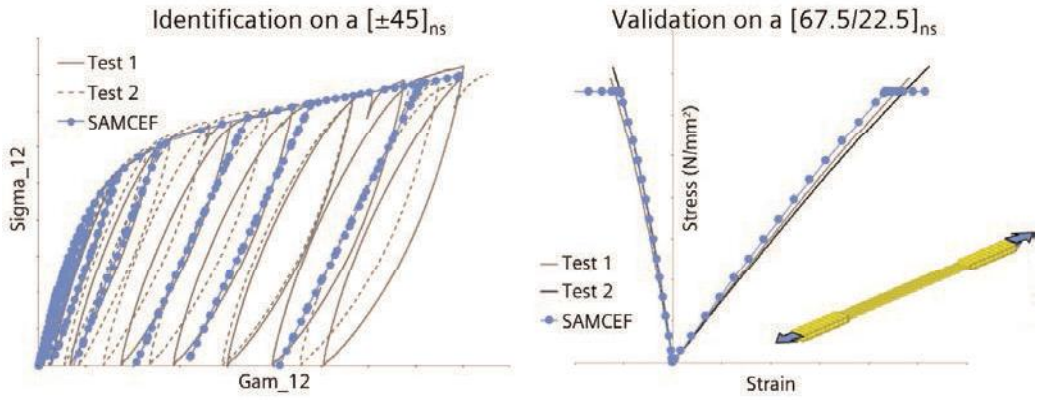


Figure 4. Comparison between test and simulation for the identification and validation a the coupon level (intra-laminar damage model)

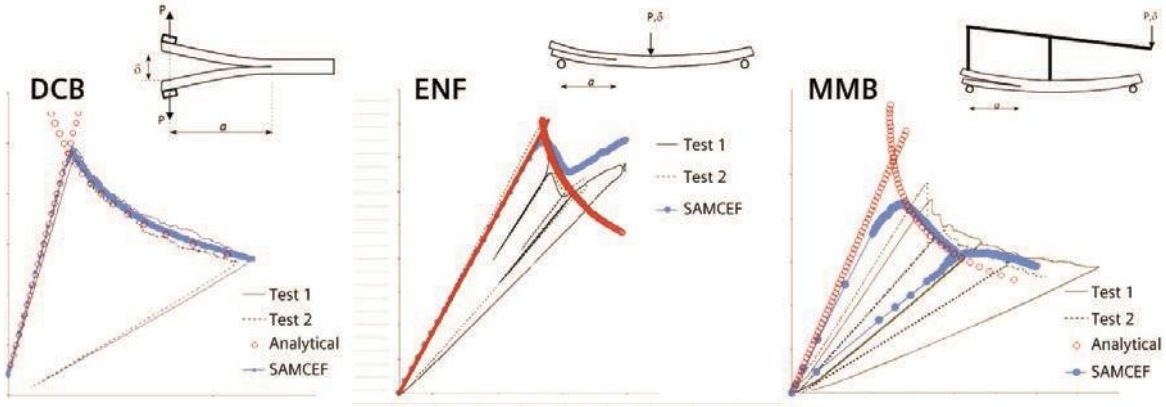


Figure 5. Comparison between test and simulation for the identification of the inter-laminar damage model parameters at the coupon level (delamination)

are illustrated in Figure 6. The agreement between test and simulation is very good.

In the second application, an L-shaped beam submitted to two different load cases and boundary conditions is considered (Figure 7). The laminates are made up of 12 plies with the following stacking sequence [60/-60/0/0/-60/60]s. Even if ply damage is present, the failure is mainly driven by delamination leading to large sliding of the plies. In Figure 8, a comparison between tests and simulations is done. The global behaviors are very similar. In Figure 9, the load-displacement curves show that a very good agreement is obtained between test and simulation.

## Fatigue Analysis of Laminated Composites

Besides the static case described in the previous sections, fatigue is another attribute to consider in the structural sizing of composites. Even if laminated composites are known to have a good behaviour in fatigue, it is anyway interesting to study for instance the degradation occurring during the first cycles as tests reveal a (possibly large) stiffness decrease during that period.

The fatigue framework available in the LMS Samtech Samcef finite element code was adapted here in order to study laminates made up of unidirectional plies submitted to intra-laminar damage. It is based on the cycle jump approach proposed in [5], and relies on the

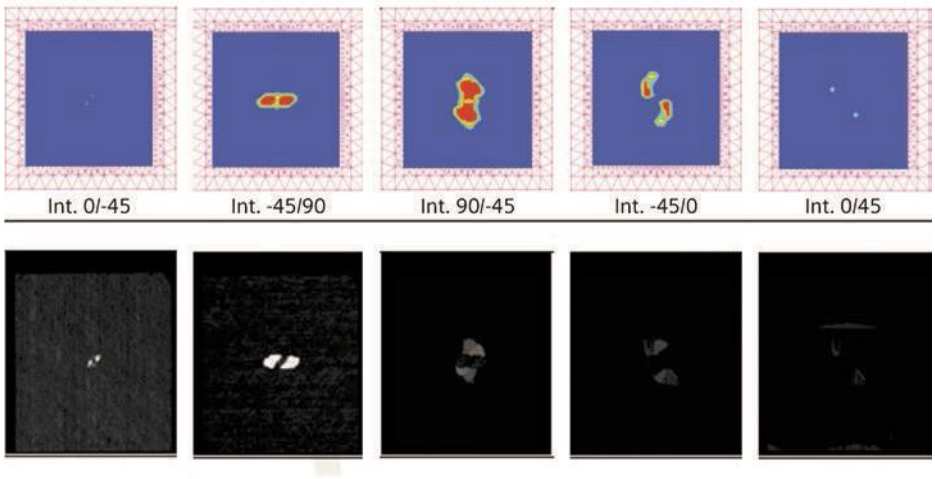


Figure 6. Results of the impact on the laminated plate

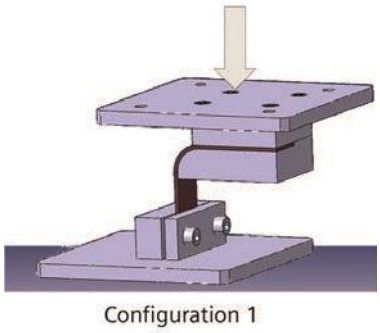


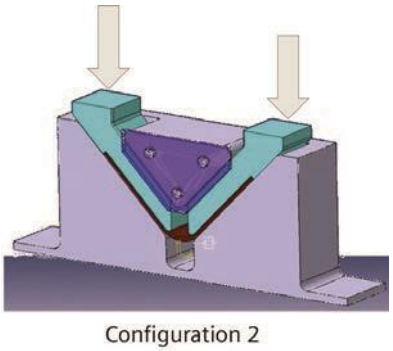


Figure 7. Two configurations for the L-shaped beam

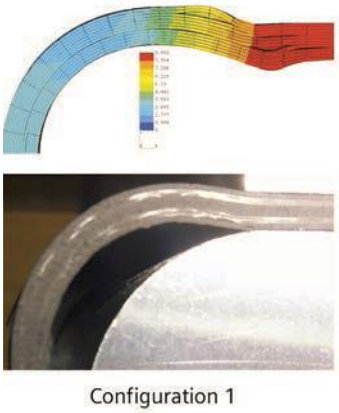


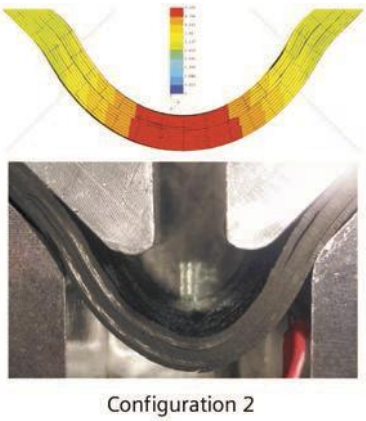


Figure 8. Delamination resulting from the loading

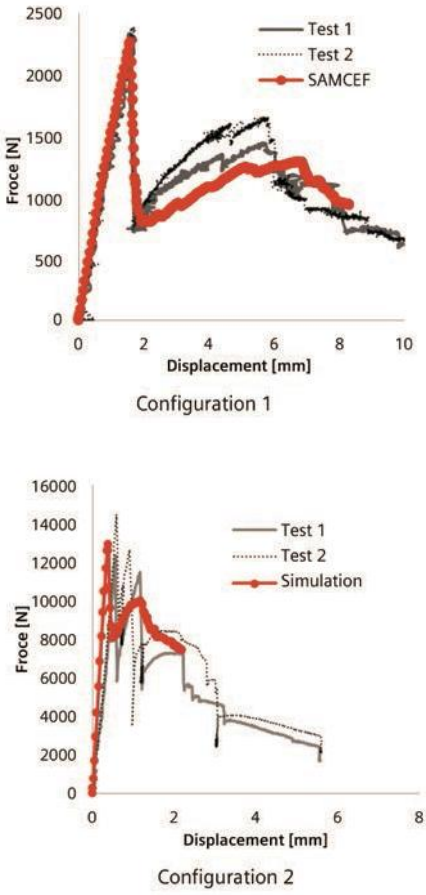


Figure 9. Load-displacement curves

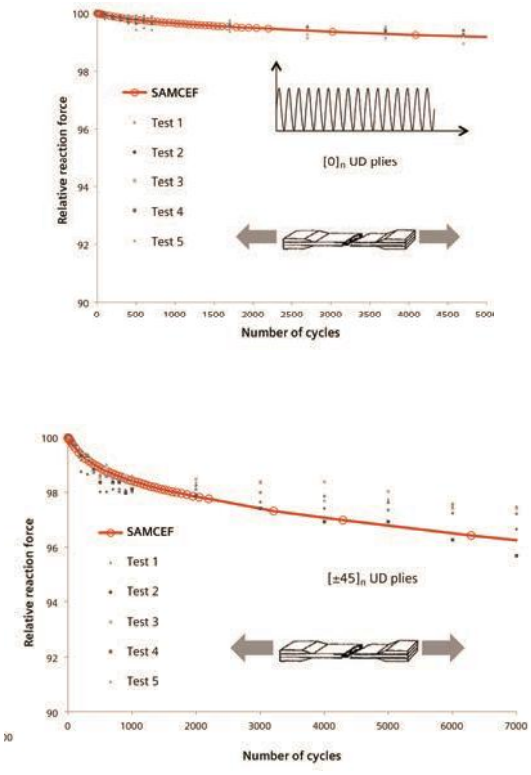


Figure 10. Fatigue in a $[0]_n$ and in a $[\pm 45]_n$

continuum damage mechanics described in the previous sections, as stiffness decrease is also observed in fatigue. In the developed formulation, the cyclic loading is limited to constant amplitude. An extension to variable amplitudes is developed in LMS Virtual Lab Durability. With the specific fatigue law $\partial d/\partial N$ (where N stands for the number of cycles) and the cycle jump strategy, the computation of each cycle is avoided, saving large computational times. In Figure 10, the resultant reaction force of the coupon submitted to a fatigue membrane loading is recorded: it decreases over time, demonstrating that damage appears in the plies. First comparisons between physical tests and simulations for intra-laminar fatigue damage appearing after few cycles in coupons made up of plies oriented at either 0° or ±45°, and submitted to membrane loading, are reported in Figure 10.

## Summary and Concluding Remarks

In this paper, we have described the damage models for laminates made up of UD plies available in the LMS Samtech Samcef finite element software. Both inter and intra-laminar damages are addressed. The formulations and the methodology were presented and the parameter identification procedure at the coupon level was explained. Very good agreements were found between tests and predictive simulations at the coupon level and at the upper stages of the pyramid.

The methodology described for laminates made up of unidirectional plies and the static case was also demonstrated for woven fabrics and NCF materials [6,7]. Solutions of aerospace applications are available in [8-10].

## References


[1] Ladeveze P., Le Dantec S. (1992). Damage modeling of the elementary ply for laminated composites, Composites Science & Technology, 43, pp. 123-134.

[2] Bruyneel M., Delsemme J.P., Goupil A.C., Jetteur P., Lequesne C., Naito T., Urushiyama Y. (2014). Damage modeling of laminated composites: validation of the intra-laminar damage law of SAMCEF at the coupon level for UD plies, European Conference on Composite Material, ECCM16, Sevilla, Spain, 22-26 June 2014.

[3] Allix O., Ladevèze P. (1992). Interlaminar interface modelling for the prediction of laminate delamination, Composite Structures, 22, pp. 235-242

[4] Bruyneel M., Delsemme J.P., Goupil A.C., Jetteur P., Lequesne C., Naito T., Urushiyama Y. (2014). Damage modeling of laminated composites: validation of the inter-laminar damage law of SAMCEF at the coupon level for UD plies, World Congress of Computational Mechanics, WCCM11, Barcelona, Spain, 20-25 July, 2014.

[5] Van Paepeghem W. (2002). Development and finite element implementation of a damage model for fatigue of fibre-reinforced polymers. PhD Thesis, University of Ghent, Belgium.

[6] Bruyneel M., Delsemme J.P., Goupil A.C., Jetteur P., Lequesne C., Naito T., Urushiyama Y. (2014). Damage modeling of woven-fabric laminates with SAMCEF: validation at the coupon level, International Conference on Advanced Computational Methods in Engineering – ACOMEN 2014, Ghent, Belgium, 23-28 June, 2014.

[7] Bruyneel M., Delsemme J.P., Jetteur P., Lequesne C., Sopelsa L., Naito T., Urushiyama Y. (2015). Validation of the LMS Samtech Samcef material models for inter- and intra-laminar damages in laminated composites made of NCF plies, ICCS18 International Conference on Composite Structures, June 15-18 2015, Lisbona, Portugal.

[8] Bruyneel M., Delsemme J.P., Jetteur P., Germain F. and Boudjemaa N. (2014). Damage modeling of composites: validation of inter-laminar damage model at the element level, JEC Composites Magazine, 90, June 2014.

[9] Bruyneel M., Degenhardt R. and Delsemme J.P. An industrial solution to simulate post-buckling and damage of composite panels, JEC Composites Magazine, 48, May 2009.

[10] Galucio A.C., Jetteur P., Trallero D., Charles J.P. Toward numerical fatigue prediction of composite structures: application to helicopter rotor blades, 3rd ECCOMAS Conference on the Mechanical Response of Composites, 21-23, Hannover, Germany, 2011.